

Interference effects due to nuclear motion of the hydrogen moleculeL. O. Santos,¹ Amanda Alencar,² I. Prazeres,² F. Impens,² J. Robert,³ C. R. de Carvalho,²
N. V. de Castro Faria,² and Ginette Jalbert^{2,*}¹*Centro de Instrução Almirante Graça Aranha, Rio de Janeiro, Rio de Janeiro 21030-001, Brazil*²*Instituto de Física, Universidade Federal do Rio de Janeiro, Caixa Postal 68528, Rio de Janeiro, Rio de Janeiro 21941-972, Brazil*³*Laboratoire Aimé Cotton CNRS, Université Paris Sud-11, ENS Cachan, 91405 Orsay, France*

(Received 23 August 2018; published 28 November 2018)

We show that two-particle interferences can be used to probe the nuclear motion in a doubly excited hydrogen molecule. The dissociation of molecular hydrogen by electron impact involves several decay channels, associated with different molecular rotational states, which produce quantum interferences in the detection of the atomic fragments. Thanks to the correlations between the angular momentum and the vibrational states of the molecule, the fragments arising from each dissociation channel carry out a phase shift which is a signature of the molecule rotation. These phase shifts, which cannot be observed in a single-atom detection scheme, may be witnessed under realistic experimental conditions in a time-of-flight coincidence measurement. We analyze the interferences arising from the two lowest-energy rotational states of a parahydrogen molecule. Our result shows the relevance of two-fragment correlations to track the molecular rotation.

DOI: [10.1103/PhysRevA.98.052136](https://doi.org/10.1103/PhysRevA.98.052136)**I. INTRODUCTION**

Two-photon correlations are essential in the modern definition of coherence [1]. In fact, two-photon interference experiments, such as the Hong-Ou-Mandel interference [2], have played a key role in the developments of quantum optics. Two-particle interference has been performed involving atoms instead of photons in a Hong-Ou-Mandel type experiment [3]. Besides, two-photon correlations can provide information about the light source beyond that obtained with a single intensity measurement [4]. On the other hand, in the dissociation of a diatomic molecule, the source of the final two-particle state is the molecule itself. Connected to this, quantum interferences have been predicted when there are at least two distinct dissociative states excited at the same energy [5] and, for instance, have been measured for photodissociation of H₂ [6] and more recently for D₂ [7]. Quantum interferences have also been reported in ionization processes [8–10] involving an asymmetric molecular fragmentation [11,12].

In this paper it is shown that two-atom correlations may provide an insight into the nuclear motion that is inaccessible to single-atom measurements; more precisely, it is theoretically foreseen an interference pattern in the superposition of the wave functions of two H(2s) fragments, which emerge from the dissociation of H₂, related to different molecular rotational states. It must be emphasized that such two-atom interferences may be observed in a standard coincidence time-of-flight detection experiment similar to the setup reported in Ref. [13] for the production of metastable H(2s) hydrogen fragments. The knowledge of the initial molecular state is important to design an experiment such as the one suggested in Ref. [14], which constitutes a potential twin-atom source.

Long-lived metastable fragments can be obtained through the H(2s) + H(2s) dissociation channel of the doubly excited states of molecular hydrogen. The production of these doubly excited states by electron impact has been recently analyzed [15]. Multiple dissociative states correspond to different angular momentum contributions of the internuclear axis rotation. Hence, the distinct dissociation paths which produce quantum interferences are labeled by different rotational states of the molecule.

The effective molecular potential felt by the nuclei couples the angular momentum of them to the vibrational state of the molecule. The phase shifts imprinted on the atomic fragments by this effective molecular potential depend on the molecule rotation. These “rotational” phases cannot be observed in an experiment involving a single atomic detector. Their difference may nevertheless be measured in a coincidence time-of-flight detection experiment involving simultaneously the two H(2s) fragments produced in the dissociation. Even though the molecular state arising from the dissociation is indeed entangled [16,17], the proposed measurement of the rotational phases does not use any specific property of entanglement.

II. THEORETICAL DESCRIPTION**A. Description of the H₂ wave function in the Born-Oppenheimer approximation**

In the Born-Oppenheimer approximation, following Refs. [18,19], the molecular wave function in the laboratory frame without spins is given by

$$\Psi_{\text{mol}} = \frac{1}{r} \sum_{J, M_J} c_{J, M_J} \psi_{\text{el}, \Lambda} \chi_{v, J} Y_J^{M_J}(\theta, \phi), \quad (1)$$

where $J = L + N$ is the total angular momentum; L and N stand for the electrons and nuclei angular momenta,

*ginette@if.ufrj.br

respectively; Λ and M_J are the projections of L and J along the internuclear axis, respectively; $\psi_{\text{el},\Lambda}$ is the electronic wave function; $\chi_{v,J}$ and $Y_{M_J}^J$ are the nuclear vibrational and rotational wave functions; and finally (θ, ϕ) are the angles of the nuclear axis with respect to the laboratory frame [18,19].

The molecular wave function must fulfill symmetry requirements in compliance with the fermionic nature of its components. In its ground state H_2 lies in the $^1\Sigma_g^+$ electronic state and it has been shown that the doubly excited state, which produces $\text{H}(2s) + \text{H}(2s)$ fragments and cannot be reached by photon excitation, has the same electronic symmetry [20]. Therefore, it leads to $L = 0$, $\Lambda = 0$, and $J = N$. It is worth mentioning that the electronic part is symmetric by the exchange of nuclei. Considering $\tilde{\Psi}_{\text{mol}} = \Psi_{\text{mol}}\xi_{\text{el}}$ as the molecular wave function plus the electronic spin (ξ_{el}) and taking into account the nuclear spin, ξ_N , one has two distinct possibilities:

$$(i) \Psi_{\text{tot}}^A = \tilde{\Psi}_{\text{mol}}^S \xi_N^A \text{ (parahydrogen),}$$

$$(ii) \Psi_{\text{tot}}^A = \tilde{\Psi}_{\text{mol}}^A \xi_N^S \text{ (orthoxygen).}$$

Therefore, for the electronic state $^1\Sigma_g^+$, one has the wave function $\tilde{\Psi}_{\text{mol}}^S$ for $J = N$ even and $\tilde{\Psi}_{\text{mol}}^A$ for $J = N$ odd. We consider only the parahydrogen configuration. Although under ordinary conditions a sample of H_2 , in its ground state, has its ortho form three times as abundant as the para one, the choice of only considering the parahydrogen corresponds nevertheless to a realistic experimental configuration as pure samples of parahydrogen can be produced with well-known techniques [21,22].

As the molecule nuclear spin state is unchanged by the electron collision, one can say that the global excited state here considered has the same symmetry as the initial ground state.

At room temperature, the ground state of the molecular hydrogen in thermal equilibrium has few rotational levels significantly populated (up to $N = 3$). Moreover, rotational transitions are not likely to happen in electron impact collisions (especially in the high-electron-impact energy range) [23]; therefore one can consider that only rotational transitions with small ΔN take place after collision. Thus, noting that we are dealing with parahydrogen, we assume that the initial rotational state is only $N = 0$ [24], leading to an excited state which is a linear combination of $N = 0$ and $N = 2$. Without the center-of-mass motion, one can write Eq. (1) as

$$\psi_{\text{mol}} = \sum_{N \in \{0,2\}, M_N} c_{N, M_N} \psi_{\text{el},0} \frac{\chi_{v,N}}{r} Y_{M_N}^N(\theta, \phi). \quad (2)$$

Instead of deriving explicitly the coefficients c_{N, M_N} associated with the collisional process, we focus on the asymptotic form of the wave function and look for the associated nuclei momentum distributions.

As we are interested in the outgoing fragments, only the outgoing contribution of the asymptotic form of the vibrational wave function $\chi_{v,N}(r \rightarrow +\infty) = e^{i(kr + 2\delta_N - \frac{N\pi}{2})}$ is retained. The associated frequency reads $h\nu = \frac{\hbar^2 k^2}{2\mu}$, where μ is the reduced mass and $\hbar k$ is the relative momentum of the nuclei and r is its relative position. One of the signatures of the repulsive potential is contained in the phase shift δ_N ,

which can be obtained by treating the dissociation process as a time-reversed collisional process.

A complete description in the laboratory frame requires one to take into account the center-of-mass motion. In this sense, it is useful to project the nuclei's momenta along the axes formed by the two detectors and to introduce the wave vectors of the nuclei:

$$k_A^\pm = \frac{K}{2} \pm k, \quad k_B^\pm = \frac{K}{2} \mp k, \quad (3)$$

where $\hbar K$ corresponds to the center of mass and $\hbar k$ to the relative momentum of the two nuclei labeled by the letters A and B . The signals $+$ and $-$ correspond to the direction of emission of the nucleus A in the center-of-mass frame. Moreover, in order to obtain a proper description of the asymptotic wave function one has to take into account all the possible relative momenta allowed in the Franck-Condon region [18]. The detection system can be designed to be sensitive exclusively to the fragments in the $|2s\rangle$ state [13]. Thus, in the asymptotic limit $r \rightarrow \infty$, the molecular wave function corresponding to the dissociation of H_2 in the state $Q_2 \ ^1\Sigma_g^+$ takes the following form:

$$\begin{aligned} \Psi_{\text{asy}} = & \sum_{N, M_N} \int dK G(K) \int dk f_N(k) e^{-\frac{iN\pi}{2}} e^{i2\delta_N} \\ & \times [\Theta(r_B - r_A) e^{i(k_A^- r_A + k_B^- r_B)} + \Theta(r_A - r_B) e^{i(k_A^+ r_A + k_B^+ r_B)}] \\ & \times (|2s\rangle_A^1 |2s\rangle_B^2 + |2s\rangle_A^2 |2s\rangle_B^1) Y_N^{M_N}(\theta, \phi), \end{aligned} \quad (4)$$

where $G(K)$ is related to the center-of-mass moment distribution and $f_N(k)$ to the relative one, which is obtained from the reflection method [25]. Note that the function $\Theta(r_i - r_j)$ (i and j standing for A and B) guarantees the correct signs of the exponentials' arguments depending on which particle goes to the left and which goes to the right. From now on we replace $Y_N^{M_N}(\theta, \phi)$ by $|N, M_N\rangle$. As we are dealing with thermal molecules whose velocities are null on average, we may consider null the molecule's center-of-mass moment, which corresponds to $G(K) = \delta(0)$; consequently, the moments of the fragments are opposite and of the same magnitude in the laboratory frame of reference as can be seen in Eq. (3).

B. Quantum description of the detection apparatus

The geometry of the detection system is depicted in Fig. 1. The detectors should be aligned to ensure that if one atom is detected, the other one, arriving from the same dissociation, is also detected by the other detector.

The propagation of the fragments occurs along the internuclear axis, so that the aperture of the detectors filters a finite solid angle Ω of the possible angular positions (θ, ϕ) . This finite aperture effect is of crucial importance, as it provides different weights for the angular momentum states $N = 0$ and 2.

Besides, there is a unique correspondence between these momenta and the time-of-flight of the fragments to the detectors. Thus, a couple of momentum eigenstates (k_A, k_B) yield well-defined arrival times (τ_A, τ_B) . As we are dealing with identical fragments, each click registered in a detector may correspond to either one of the fragments.

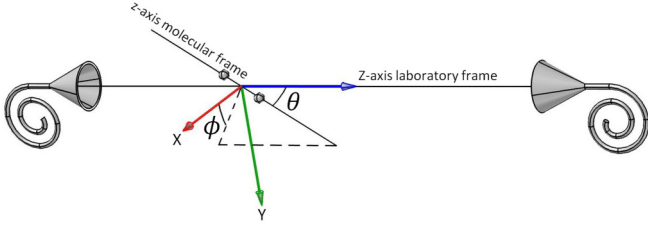


FIG. 1. The Z axis in laboratory frame is defined by the line crossing the center of both detectors. The variables (θ, ϕ) are the angles of the nuclear axis with respect to the laboratory frame and, as it is mentioned in the text, (Θ, Φ) corresponds to the detector's solid angle Ω .

Summing up these considerations, one may think of the detectors in terms of projection operators in the momentum and angular (detector's solid angle Ω) spaces, and a transition operator from the $2s$ to the $1s$ electronic state, with the latter corresponding to the process that takes place in the detection. Therefore

$$\begin{aligned} \hat{D}_r = & [\mathbb{I}_A \otimes \langle k_r \rangle_B |1s\rangle_{BB} \langle k_r |_B \langle 2s| \\ & + \langle k_r \rangle_A |1s\rangle_{AA} \langle k_r |_A \langle 2s| \otimes \mathbb{I}_B] \\ & \times \int_{\Omega} d\Omega |\Theta, \Phi\rangle \langle \Theta, \Phi|, \end{aligned} \quad (5)$$

where subscript r stands for right side detection. For example, when \hat{D}_r acts on atom B , its linear momentum k is detected. For the left side one has a similar expression for \hat{D}_l . Detection in coincidence corresponds to the application of both operators \hat{D}_l and \hat{D}_r .

The counting number in each detector (the probability per unit of momentum) is proportional to $P_i = \langle \Psi_{\text{asy}} | \hat{D}_i^\dagger \hat{D}_i | \Psi_{\text{asy}} \rangle$, where $i = l$ or r depending on which side is addressed. Analogously the detection in coincidence is proportional to

$$P_{\text{coinc}} = \langle \Psi_{\text{asy}} | \hat{D}_l^\dagger \hat{D}_r^\dagger \hat{D}_l \hat{D}_r | \Psi_{\text{asy}} \rangle = |\hat{D}_l \hat{D}_r \Psi_{\text{asy}}^P|^2.$$

III. RESULTS AND DISCUSSION

As we consider the parahydrogen with $N = 0$ and $N = 2$, we obtain the following from Eqs. (4) and (5):

$$\begin{aligned} & |\hat{D}_l \hat{D}_r \Psi_{\text{asy}}^P|^2 \\ & = 2 \left\{ f_0^2(k_r) \int_{\Omega_\cap} d\Omega \langle 0, 0 | \Theta, \Phi \rangle \langle \Theta, \Phi | 0, 0 \rangle \right. \\ & \quad + f_2^2(k_r) \sum_{M_2, M_2'} \int_{\Omega_\cap} d\Omega \langle 2, M_2' | \Theta, \Phi \rangle \langle \Theta, \Phi | 2, M_2 \rangle \\ & \quad - 2 \left[f_2(k_r) f_0(k_r) \cos[2(\delta_2 - \delta_0)] \right. \\ & \quad \left. \left. \times \sum_{M_2} \int_{\Omega_\cap} d\Omega \langle 0, 0 | \Theta, \Phi \rangle \langle \Theta, \Phi | 2, M_2 \rangle \right] \right\}, \end{aligned} \quad (6)$$

where Ω_\cap is the solid angle of the detector that is farthest from the dissociation region. For this reason, the integral of Eq. (6)

must be performed for the smaller solid angle between the two detectors.

In the case of simple detection, one can show that

$$|\hat{D}_r \Psi_{\text{asy}}|^2 = \frac{\Omega}{2\pi} \sum_{N, M_N} f_N^2(k_r), \quad (7)$$

which reflects the fact that one has no privileged axis of detection. Unlike that, in coincidence measurement one has a privileged axis formed by the line of the two detectors. This means that the integral of the third term in Eq. (6) does not vanish. The first two terms of Eq. (6) are similar to the ones obtained in the simple detection case. On the other hand, the third one corresponds to an *interference term* between the two possible paths in the dissociation of the molecule.

The phase shifts in Eq. (6) (see the Appendix) were obtained by modifying a code written by Canto and Hussein [26] aimed at nuclear systems and changed to systems of molecular physics. In this code δ_0 and δ_2 are obtained as a function of the kinetic energy of the fragments, E (eV).

For the numerical analysis of the coincidence detection, we consider that the two detectors are aligned with respect to the dissociation region and that the farthest detector is at 21 cm from this region, while the nearest detector is 18 cm away from the dissociation region. As the detectors are aligned, the solid angle Ω_\cap considered will be the one associated with the detector that is farther from the dissociation region (at 21 cm).

The connection between the relative momentum k and the difference in time-of-flight Δt of each atom is given by $k = 2(\mu/\hbar)(\Delta l/\Delta t)$, where $\Delta l = l_l - l_r$ is the modulus of the difference between the distances traveled by the atoms from the dissociation region to their detection by the detectors \hat{D}_l and \hat{D}_r , respectively.

In order to conciliate the theory, expressed by $|\hat{D}_e \hat{D}_d \Psi_{\text{asy}}|^2$, with the experimental counting rate, the following transformation is necessary:

$$|\hat{D}_e \hat{D}_d \Psi_{\text{asy}}|^2 dk = h_c(\Delta t) d\Delta t. \quad (8)$$

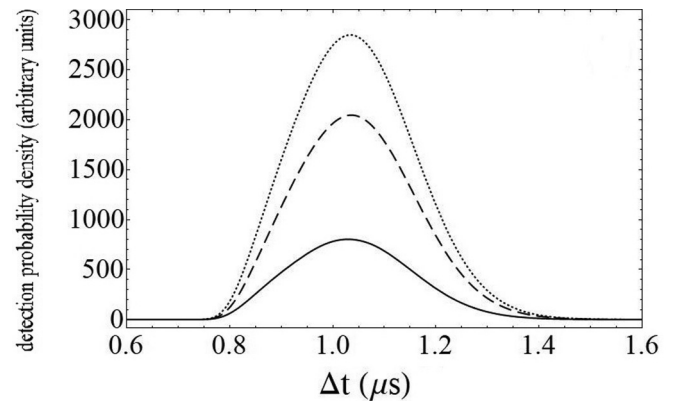


FIG. 2. Detection in coincidence, in arbitrary units, as a function of Δt . This figure presents the probability density of detection $h_c(\Delta t)$ [solid line, Eq. (8)], the probability density of detection without the interference term (dotted line), and the module of the interference term (dashed line). Both detectors are aligned relative to the dissociation region, with one of them spaced 18 cm apart from this region and the other one 21 cm apart.

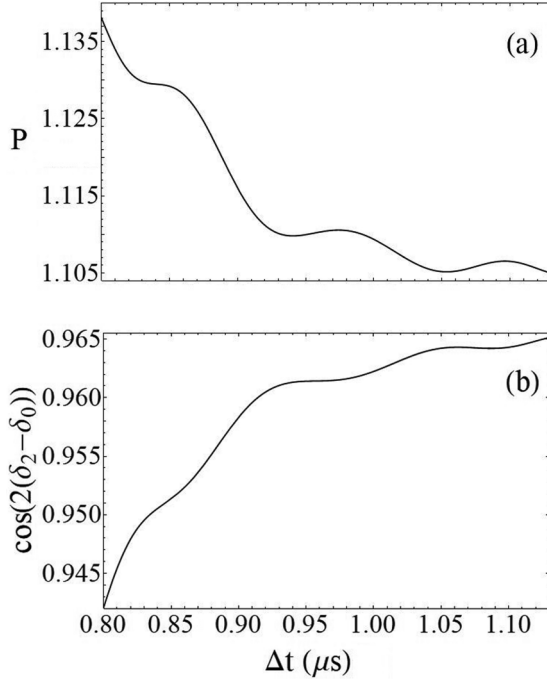


FIG. 3. (a) Oscillation of the normalized counting rate $P(\Delta t)$; (b) $\cos[2(\delta_2 - \delta_0)]$ as a function of Δt . For details, see the text.

Figure 2 shows $h_c(\Delta t)$, in arbitrary units, obtained from Eq. (8), together with the contribution originated from the two first terms of Eq. (6) (dotted line) and the modulus of the third one, the interference term (dashed line). The main difference between the probability density with and without interference is related to the amplitude, although the two distributions are slightly shifted.

Despite the presence of the interference term, it is not possible to observe oscillatory behavior in $h_c(t)$, as shown in Fig. 2. This is due to the fact that the oscillations which arise from $\cos[2(\delta_2 - \delta_0)]$ are quite small in the energy range of interest, fixed by the Franck-Condon region.

To enhance the phase-shift difference effect in the interference term of Eq. (6), we divide the Eq. (6) by

$$\begin{aligned}
 p(k_r) = & 2 \left\{ f_0^2(k_r) \int_{\Omega_\cap} d\Omega \langle 0, 0 | \Theta, \Phi \rangle \langle \Theta, \Phi | 0, 0 \rangle \right. \\
 & + f_2^2(k_r) \sum_{M_2, M_2'} \int_{\Omega_\cap} d\Omega \langle 2, M_2' | \Theta, \Phi \rangle \langle \Theta, \Phi | 2, M_2 \rangle \\
 & \left. - 2 \left[f_2(k_r) f_0(k_r) \sum_{M_2} \int_{\Omega_\cap} d\Omega \langle 0, 0 | \Theta, \Phi \rangle \langle \Theta, \Phi | 2, M_2 \rangle \right] \right\} \quad (9)
 \end{aligned}$$

and then convert the result in terms of Δt . The behavior of the resulting expression, $P(\Delta t)$, is displayed in Fig. 3(a). It is worth mentioning that Eq. (9) is equal to Eq. (6), except for the replacement of $\cos[2(\delta_2 - \delta_0)]$ by 1. The quantity $P(\Delta t) = p(\Delta t)/h_c(\Delta t)$ plays the role of a normalized counting rate and allows us to see oscillations from the result of the detection in coincidence.

It is important to notice that this *normalization* does not introduce oscillatory behavior in $P(\Delta t)$, depicted in Fig. 3(a), since $p(k_r)$ does not contain the information carried by the phase shifts. In a way, by doing the division of $|\hat{D}_l \hat{D}_r \Psi_{\text{asy}}^P|^2$ by $p(k_r)$, we remove from the data all information concerning every aspect of the system other than the phase-shift difference effect. In fact, comparing $P(\Delta t)$ with $\cos[2(\delta_2 - \delta_0)]$ in Fig. 3, we can see that their oscillations are completely connected.

IV. CONCLUSION

In this paper we have shown that, through the coincidence detection of the H(2s) atoms coming from the same H₂ molecule dissociation, it is possible to observe interference patterns due to different possible fragmentation paths in the dissociation process; this behavior is connected with the phase shifts imprinted by the repulsive effective molecular potential and reveals the coupling between the angular momentum and the vibrational states of the molecule. This result is foreseen for the data obtained in an ordinary coincidence time-of-flight detection experiment. It is also verified that this behavior cannot be observed in an experiment involving only a single detector.

ACKNOWLEDGMENTS

We thank L. F. Canto for his assistance with the application of his code to compute the phase shifts. This work was partially supported by the Brazilian agencies CNPq, CAPES, and FAPERJ. It is part of the INCT-IQ from CNPq.

APPENDIX: THE PHASE SHIFT δ_N

We detail below the method used to calculate the dissociation phase shifts δ_N involved in Eq. (6). We proceed by treating the molecule dissociation process as a “reverse collision,” in which the projectile and the target are the nuclei arising from the dissociation. Within the Born-Oppenheimer approximation, the vibrational wave function is a solution of the differential equation

$$\left[\frac{d^2}{d\rho^2} + 1 - \frac{N(N+1)}{\rho^2} \right] u_N(k, \rho) = U(k, \rho) u_N(k, \rho), \quad (\text{A1})$$

where $\rho \equiv kr$.

For $\rho > \bar{\rho}$, the interaction potential $U(k, \rho)$ vanishes. This leads us to consider two different domains: domain I ($\rho < \bar{\rho}$) associated with a nonzero interaction potential for which a numerical solution is required, and domain II ($\rho > \bar{\rho}$) corresponding to a free propagation of the fragments. In the second domain, Eq. (A1) takes the simple form

$$\left[\frac{d^2}{d\rho^2} + 1 - \frac{N(N+1)}{\rho^2} \right] u_N(k, \rho) = 0, \quad (\text{A2})$$

whose solutions can be expressed in terms of Ricatti-Bessel functions:

$$u_N(k, \rho) = \alpha_N [\hat{j}_N(\rho) + \beta_N \hat{n}_N(\rho)], \quad (\text{A3})$$

where α_N is a global constant of normalization and, for convenience, β_N can be written in terms of the phase shift δ_N as $\beta_N = \tan\delta_N$.

By linearity of Eq. (A1), any linear combination of Bessel and Neumann functions is also a solution. Thus, one may also conveniently express the wave function in terms of Ricatti-Haenkel functions:

$$u_N(k, \rho) = \alpha'_N [\hat{h}_N^{(-)}(\rho) - S_N \hat{h}_N^{(+)}(\rho)], \quad (\text{A4})$$

where $\alpha'_N = i e^{-i\delta_N} \alpha_N / \cos\delta_N$ is just a new constant of normalization and $S_N = e^{i2\delta_N}$.

Within domain I the vibrational differential equation is solved numerically (e.g., with the Runge-Kutta method). The numerical solution (in fact, its logarithmic derivative $\mathcal{L} \equiv \frac{u'_N(k, \rho)}{u_N(k, \rho)}$) must be chosen so as to ensure the continuity of the wave function and its spatial derivative throughout the whole space. This condition imposes that the logarithmic derivatives must match across the boundary of domain I and domain II, i.e., $\mathcal{L}^I = \mathcal{L}^{II}$. Finally, this boundary condition determines the phase shift δ_N as

$$S_N = \left[\frac{\hat{h}_N^{(-)}(\bar{\rho}) - \hat{h}_N^{(-)}(\bar{\rho}) \mathcal{L}^I}{\hat{h}_N^{(+)}(\bar{\rho}) - \hat{h}_N^{(+)}(\bar{\rho}) \mathcal{L}^I} \right]. \quad (\text{A5})$$

-
- [1] R. J. Glauber, *Phys. Rev.* **130**, 2529 (1963).
 [2] C. K. Hong, Z. Y. Ou, and L. Mandel, *Phys. Rev. Lett.* **59**, 2044 (1987).
 [3] R. Lopes, A. Imanaliev, A. Aspect, M. Cheneau, D. Boiron, and C. I. Westbrook, *Nature (London)* **520**, 66 (2015).
 [4] C. Jurczak, K. Sengstock, R. Kaiser, N. Vansteenkiste, C. I. Westbrook, and A. Aspect, *Opt. Commun.* **115**, 480 (1995).
 [5] J. A. Beswick and M. Glass-Maujean, *Phys. Rev. A* **35**, 3339 (1987).
 [6] M. Glass-Maujean, H. Frohlich, and J. A. Beswick, *Phys. Rev. Lett.* **61**, 157 (1988).
 [7] J. Wang, Q. Meng, and Y. Mo, *Phys. Rev. Lett.* **119**, 053002 (2017).
 [8] D. Akoury *et al.*, *Science* **318**, 949 (2007).
 [9] B. Zimmermann *et al.*, *Nat. Phys.* **4**, 649 (2008).
 [10] M. S. Schoeffler *et al.*, *New J. Phys.* **13**, 095013 (2011).
 [11] F. Martín *et al.*, *Science* **315**, 629 (2007).
 [12] M. S. Schoeffler *et al.*, *Science* **320**, 920 (2008).
 [13] J. Robert, F. Zappa, C. R. de Carvalho, G. Jalbert, R. F. Nascimento, A. Trimeche, O. Dulieu, A. Medina, C. Carvalho, and N. V. de Castro Faria, *Phys. Rev. Lett.* **111**, 183203 (2013).
 [14] C. R. de Carvalho, G. Jalbert, F. Impens, J. Robert, A. Medina, F. Zappa, and N. V. de Castro Faria, *Europhys. Lett.* **110**, 50001 (2015).
 [15] L. O. Santos, A. B. Rocha, N. V. de Castro Faria, and G. Jalbert, *Eur. Phys. J. D* **71**, 1 (2017).
 [16] T. Opatrný and G. Kurizki, *Phys. Rev. Lett.* **86**, 3180 (2001).
 [17] D. Petrosyan, G. Kurizki, and M. Shapiro, *Phys. Rev. A* **67**, 012318 (2003).
 [18] B. H. Bransden and C. J. Joachain, *Physics of Atoms and Molecules* (Wiley & Sons, New York, 1990).
 [19] L. D. A. Siebbeles, J. M. Schins, W. J. van der Zande, and J. A. Beswick, *Chem. Phys. Lett.* **187**, 633 (1991).
 [20] L. O. Santos, A. B. Rocha, R. F. Nascimento, N. V. de Castro Faria, and G. Jalbert, *J. Phys. B: At. Mol. Opt. Phys.* **48**, 185104 (2015).
 [21] R. B. Leighton, *Principles of Modern Physics* (McGraw-Hill, New York, 1959).
 [22] F. T. Wall, *Chemical Thermodynamics* (Freeman, S. Francisco, 1974).
 [23] Yu. D. Oksyuk, *J. Exp. Theor. Phys. (U.S.S.R.)* **49**, 1261 (1965) [*Sov. Phys. JETP* **22**, 873 (1966)].
 [24] The initial state may contain higher rotational terms ($N > 0$). However, the presence of such terms would merely change the values of the coefficients c_{N, M_N} involved in Eq. (2) without affecting the general expression of the interference pattern.
 [25] A. Medina, G. Rahmat, C. R. de Carvalho, G. Jalbert, F. Zappa, R. F. Nascimento, R. Cireasa, N. Vanhaecke, I. F. Schneider, N. V. de Castro Faria, and J. Robert, *J. Phys. B: At. Mol. Opt. Phys.* **44**, 215203 (2011).
 [26] L. F. Canto and M. S. Hussein, *Scattering Theory of Molecules, Atoms and Nuclei* (World Scientific, Singapore, 2013).